Chemical Physics Letters 703 (2018) 112–116

Contents lists available at ScienceDirect

Chemical Physics Letters

journal homepage: www.elsevier.com/locate/cplett

Research paper

Two-photon absorption of soft X-ray free electron laser radiation by graphite near the carbon K-absorption edge

Royce K. Lam [a,b], Sumana L. Raj [a], Tod A. Pascal [c], C.D. Pemmaraju [d], Laura Foglia [e], Alberto Simoncig [e], Nicola Fabris [f,g], Paolo Miotti [f,g], Christopher J. Hull [a,b], Anthony M. Rizzuto [a,b], Jacob W. Smith [a,b], Riccardo Mincigrucci [e], Claudio Masciovecchio [e], Alessandro Gessini [e], Giovanni De Ninno [e,h], Bruno Diviacco [e], Eleonore Roussel [e], Simone Spampinati [e], Giuseppe Penco [e], Simone Di Mitri [e], Mauro Trovò [e], Miltcho B. Danailov [e], Steven T. Christensen [i], Dimosthenis Sokaras [j], Tsu-Chien Weng [k], Marcello Coreno [e,l], Luca Poletto [f], Walter S. Drisdell [b], David Prendergast [c], Luca Giannessi [e,m], Emiliano Principi [e], Dennis Nordlund [j], Richard J. Saykally [a,b,*], Craig P. Schwartz [c,j,*]

[a] Department of Chemistry, University of California, Berkeley, CA 94720, USA
[b] Chemical Sciences Division, Lawrence Berkeley National Laboratory, Berkeley, CA 94720, USA
[c] The Molecular Foundry, Lawrence Berkeley National Laboratory, Berkeley, CA 94720, USA
[d] Theory Institute for Materials and Energy Spectroscopies, SLAC National Accelerator Laboratory, Menlo Park, CA 94025, USA
[e] Elettra-Sincrotrone Trieste S.C.p.A., Strada Statale 14 – km 163.5, 34149 Trieste, Italy
[f] Institute of Photonics and Nanotechnologies, National Research Council of Italy, via Trasea 7, I-35131 Padova, Italy
[g] Department of Information Engineering, University of Padova, via Gradenigo 6/B, I-35131 Padova, Italy
[h] Laboratory of Quantum Optics, University of Nova Gorica, 5001 Nova Gorica, Slovenia
[i] National Renewable Energy Laboratory, Golden, CO 80401, USA
[j] SLAC National Accelerator Laboratory, Menlo Park, CA 94025, USA
[k] Center for High Pressure Science & Technology Advanced Research, Pudong, Shanghai 201203, China
[l] ISM-CNR, Elettra Laboratory, Basovizza, I-34149 Trieste, Italy
[m] ENEA, C.R. Frascati, Via E. Fermi 45, 00044 Frascati (Rome), Italy

ARTICLE INFO

Article history:
Received 5 January 2018
In final form 9 May 2018
Available online 16 May 2018

ABSTRACT

We have examined the transmission of soft X-ray pulses from the FERMI free electron laser through carbon films of varying thickness, quantifying nonlinear effects of pulses above and below the carbon K-edge. At typical of soft X-ray free electron laser intensities, pulses exhibit linear absorption at photon energies above and below the K-edge, ~308 and ~260 eV, respectively; whereas two-photon absorption becomes significant slightly below the K-edge, ~284.2 eV. The measured two-photon absorption cross section at 284.18 eV ($\sim 6 \times 10^{-48}$ cm^4 s) is 7 orders of magnitude above what is expected from a simple theory based on hydrogen-like atoms – a result of resonance effects.

1. Introduction

The development of ultrafast lasers capable of producing pulses with high energies and peak powers has enabled the general study of matter by nonlinear spectroscopic methods [1,2]. While this field has heretofore been limited to optical wavelengths, extension to X-ray wavelengths promises to provide an element- and chemical-specific probe, capable of yielding vital new information [3,4]. However, the lack of high peak power X-ray light sources with requisite spatio-temporal coherence has thus far precluded the study of nonlinear effects at those energies [5]. Very recently, the advent of X-ray free electron lasers (FELs) has extended the field of nonlinear optics [6] to X-ray wavelengths and FELs have been used to further the understanding of X-ray-induced lasing processes[7], transient gratings [8], second harmonic generation [9,10], and sum frequency generation [11].

Two-photon absorption (TPA), wherein two photons are absorbed simultaneously, is a fundamental third-order nonlinear optical process (shown schematically in the inset of Fig. 1) [12]. Since being demonstrated in the 1960s [13], TPA has been widely exploited, from initializing polymerization for 3D data storage [14] to microscopy in biological systems [15]. In contrast to optical

* Corresponding authors at: Department of Chemistry, University of California, Berkeley, CA 94720, USA (R.J. Saykally). The Molecular Foundry, Lawrence Berkeley National Laboratory, Berkeley, CA 94720, USA (C.P. Schwartz).

E-mail addresses: saykally@berkeley.edu (R.J. Saykally), cpschwartz@lbl.gov (C.P. Schwartz).

https://doi.org/10.1016/j.cplett.2018.05.021
0009-2614/

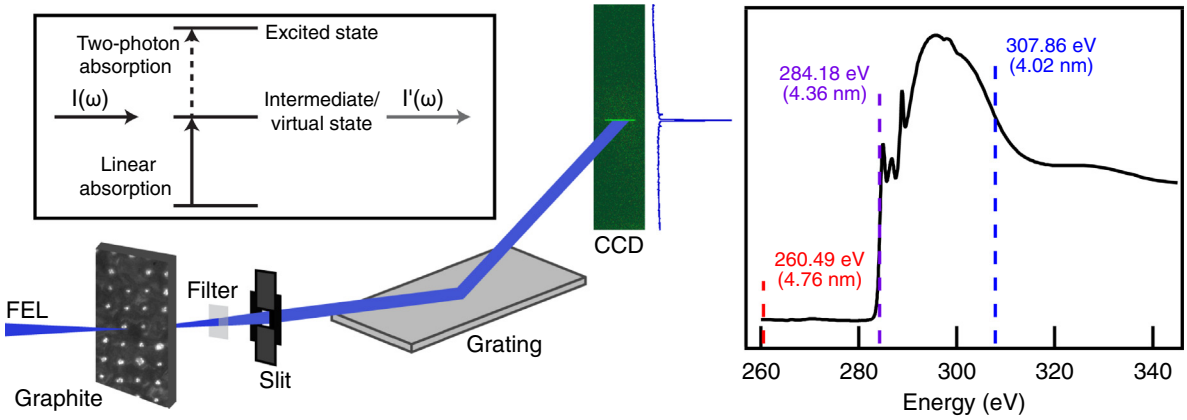

Fig. 1. Experimental schematic. X-ray pulses from the FEL are focused and either intercepted by a sample or allowed to transmit, before being dispersed by a grating and imaged by a camera. This design permits a direct determination of transmission. **Right:** Linear, total electron yield, spectrum for a 500 nm graphite sample. X-ray TPA measurements were conducted at 3 discrete photon energies show in the dashed lines. **Inset:** Schematic of the dominant processes observed in this work, two-photon absorption. While linear (one-photon) absorption is always present, the rate of two-photon absorption is particularly sensitive to the absorption edge and the nature of the excited state. Only the lowest energy studied here is a virtual state. $I_0(\omega)$ and $I(\omega)$ represent the intensity of the input (I_{NS}) and transmitted beams (I_S/I_{NS}), respectively.

TPA, core-level TPA is very sensitive to the energy of the photon relative to the sample absorption edge and is element specific [16]. This has been studied previously for core-level absorption in zirconium [16], germanium [17], and copper [18] solids as well as neon [19], helium [20], and hydrogen gases [21,22]. These studies showed that TPA scales as Z^{-6} (where Z is the atomic number), with large increases in cross section as one approaches an electronic core-level absorption edge [23]. As such, the effects of TPA will need to be taken into account when conducting transmission experiments that utilize light sources capable of generating strong radiation fields, such as X-ray FELs. Furthermore, TPA has different selection rules, enabling transitions to electronic states of matter which are dipole-forbidden and thus inaccessible by conventional X-ray absorption methods. Here, we demonstrate that soft X-ray TPA in carbon is consistent with recent studies performed at hard X-ray energies, demonstrating that significant TPA is observed near the carbon K-absorption edge.

2. Experimental

2.1. Experimental design

Soft X-ray transmission experiments were performed at EIS-TIMEX at the FERMI FEL-2 free electron laser in Trieste [24–27]. FEL-2 is based on a double high gain harmonic generation (HGHG) conversion scheme wherein the first stage of the FEL serves as a pump for the second stage. The FEL beam was propagated along the Photon Analysis, Delivery, and Reduction System (PADReS), which includes shot-to-shot photon diagnostics (I_0 monitor, PRESTO (Pulse-Resolved Energy Spectrometer (Transparent and Online))) and a gas attenuator (6 m, N_2, 1.7 mbar) to remove the first stage FEL radiation [28]. The pulses were then passed through a 2 mm iris to attenuate off-axis emission and focused by an ellipsoidal mirror to a spot size of ~350 μm^2. The drain current from the ellipsoidal mirror served as an additional I_0 monitor. Photon energies of 260.49 eV, 284.18 eV, and 307.86 eV with a pulse duration ~25 fs (FWHM) were used. In an FEL source optimized for maximum peak intensity, the frequency upshift from the HGHG process can shorten the pulse duration by a factor of $\sim 7/(6n^{1/3})$, where n is harmonic number. For a 2 stage HGHG process, the pulse duration can therefore be estimated as $(7/6)^2/(nm)^{1/3}$, where m is the harmonic in the 2nd stage [29]. The wavelengths used here correspond to harmonic orders $n = 11$, 12, and 13 for the 1st stage, and $m = 5$ for the second stage. For the seed laser duration of ~67 fs employed here, this results a X-ray pulse duration of ~25 fs. Typical flux values were between 10^{26} and 10^{30} photons cm^{-2} s^{-1} for a given shot. At the laser focus, samples could be inserted (called "sample" herein) or removed (called "no sample" herein). Unsupported nanocrystalline graphite films (thickness: 100, 300, 500 nm) mounted onto L1.0 rings (10 mm diameter) from Lebow company (Goleta, CA) were used as targets. The linear, total electron yield, spectrum of a 500 nm film is shown on the right in Fig. 1. The films were rastered between each laser shot to ensure that a pristine sample was probed. The transmitted beam was propagated through a 600 nm Al filter to prevent camera saturation, onto a grating in first order (Hitachi cod. 001-0450, 2400 gr/mm central groove density), and finally onto a Princeton Instruments PIXIS-XO 400B CCD camera [30]. The use of a spectrometer enables the spatial separation of the transmitted fundamental FEL beam from the concomitant higher order radiation from the FEL and the expected X-ray emission signal from the graphite sample allowing for the direct characterization of TPA without contamination from other competing effects such as the reabsorption of soft X-ray emission which has been observed at X-ray FEL fluences [31]. A single image was recorded for each pulse. The experimental design is shown schematically in Fig. 1.

2.2. Data Analysis

Each dataset comprises hundreds of FEL pulses. The number of photons transmitted is calculated from the signal measured on the CCD, scaling for the transmission through the 600 nm Al filter and the spectrometer efficiency (entrance slits, grating, detector) [32]. The number of input photons is similarly determined with the sample removed and correlated to the drain current measured from the ellipsoidal focusing mirror immediately upstream of the sample. The established relationship enables the determination of the number of input photons with the sample present. The points were binned and the ratio between the number of photons detected with and without samples is plotted against the X-ray intensity (photons cm^{-2} s^{-1}).

The transmission through a sample for a single photon event is given as

$$\frac{I_S}{I_{NS}} = e^{-\alpha c x} \quad (1)$$

where I_S is the signal intensity with a sample and I_{NS} is the signal intensity with no sample, α is the absorption coefficient (cm^2/g),

c is the density of the material (g/cm^3), and x is the thickness (cm). As both the thickness and density can be assumed constant, the absorption ($A = \alpha cx$) should be constant for a given sample. For two-photon events the ratio is given as

$$\frac{I_S}{I_{NS}} = \frac{1}{1 + \beta c x I_{NS}} \tag{2}$$

where β is the two-photon absorption coefficient. As β is constant for a given energy and the density and thickness do not change for a given sample, βcx will be constant for a given sample. Thus, when both one-photon and two-photon absorption occur, the total ratio should be

$$\frac{I_S}{I_{NS}} = \frac{a}{1 + b * I_{NS}} \tag{3}$$

where $a = e^{-\alpha cx}$ (linear absorption) and $b = \beta cx$ (two-photon absorption) [12]. The two-photon absorption cross section was determined by following an established procedure described in the literature [16,18].

Note that the two-photon absorption data are significantly less sensitive to the quality of the laser pulse than are other nonlinear processes (e.g., second harmonic generation) [10], and so this effect can be observed without filtering based on lasing mode.

3. Results and discussion

The soft X-ray transmission through the sample at 260.49 eV, 284.18 eV, and 307.86 eV measured as a function of intensity and sample thickness is shown in Fig. 2A, B, and C respectively. The sample thicknesses shown are 100 nm (green circles), 300 nm (blue diamonds) and 500 nm (red squares). The average value of the measured transmission for a given sample thickness is shown with dashed lines, and a curve fit to Eq. (3) is shown using solid lines. Aside from the expected lower transmission, no significant effects are observed as a function of increasing sample thickness.

Transmission is sensitive to nonlinear processes both above and below the K-edge resonance. In both Fig. 2A and C, the transmission is roughly constant as a function of X-ray intensity. This implies that there are no significant nonlinear absorption effects at these energies (260.49 eV and 307.86 eV), suggesting that, at the intensities employed here (<10^{30} photons cm^{-2} s^{-1}), the current generation of soft X-ray FELs can be used off-resonance near the carbon K-edge as a probe of linear processes without concern for nonlinear processes affecting absorption cross sections. While other effects like harmonic generation and saturation are possible, the setup here allows such possibilities to be eliminated [10]. Further effects such as those seen due to reabsorption of soft X-ray emission are unlikely to be the cause of the effects seen here [31]. As the absolute linear cross section is significantly higher at 307.86 eV than at 284.18 eV, one would expect reabsorption effects to be visible at 307.86 eV, but it is not found in this work.

We note that the *nonresonant* two-photon absorption cross section as previously derived [16] would be

$$\sigma_{TPA}(Z) = 1.27 \times 10^{-50}\ Z^{-6}\ \text{cm}^4\ \text{s} \tag{4}$$

where Z is the atomic number and $\sigma_{TPA}(Z)$ is the nonresonant cross section (related to b from Eq. (3)). The calculated value, from evaluation of Eq. (4) with Z_{carbon} = 6, of 2.72×10^{-55} cm^4 s is 7 orders of magnitude smaller than the experimental value found on resonance here (6×10^{-48} cm^4 s). The effects of two-photon absorption are only observed when the laser is on-resonance, just below the graphite $1s \rightarrow \pi^*$ peak at 284.18 eV, as shown in Fig. 2B. At lower X-ray intensities, the transmission through the sample is roughly constant. However, above a threshold (~10^{27} photons cm^{-2} s^{-1}) a gradual decrease in transmission due to two-photon absorption is observed. The shape of the curves matches well with that predicted for two-photon absorption (Eq. (3)) at both 300 nm and 500 nm sample thicknesses. A more accurate cross section prediction closer to resonance would be [18]

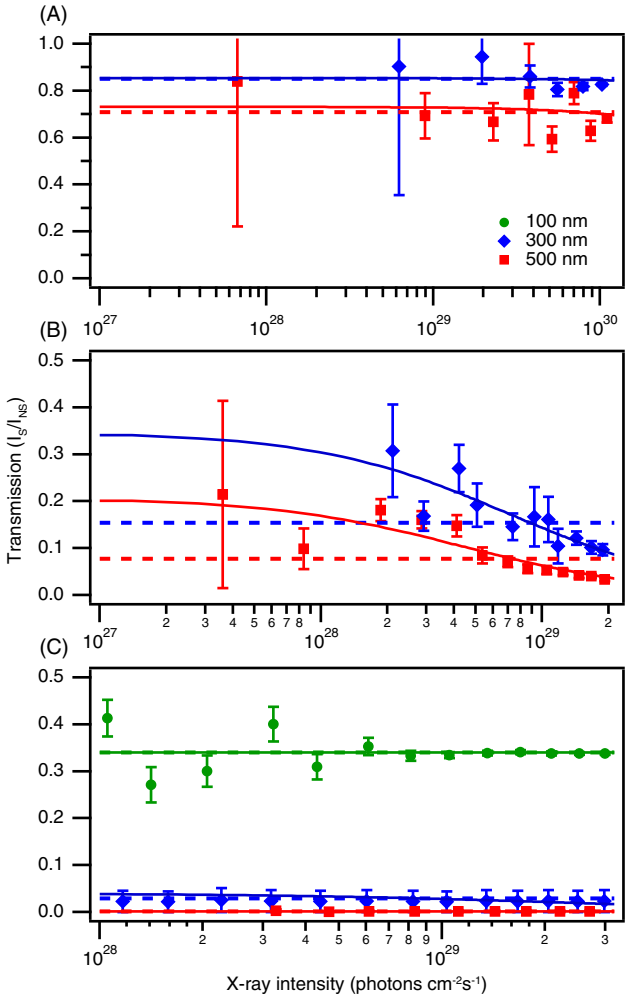

Fig. 2. Plot of the transmission versus X-ray beam intensity (log scale) at (A) 260.49 eV, (B) 284.18 eV and (C) 307.86 eV. Different sample thicknesses are shown: 100 nm (green circles), 300 nm (blue diamonds) and 500 nm (red squares). Average values of the points shown are represented by the dashed lines, while the two-photon absorption fit discussed in the text is shown as a solid line. Only at 284.18 eV is a large difference seen between the average value and the fitted curve. This is due to two-photon absorption. The log scale highlights the transition from the linear to nonlinear regimes. The samples are thin enough to enable transmission measurements. (For interpretation of the references to colour in this figure legend, the reader is referred to the web version of this article.)

$$\sigma_{TPA}(Z, E_i) = 4 \times 10^{-52}\ Z^{-4} \frac{E_i}{E_i - E_1} (\text{cm}^4\ \text{s}) \tag{5}$$

where E_1 is the binding energy – 284.2 eV for the C *1s* [32] – and E_i is the input photon energy taken from the literature. The effects of being near the absorption edge has previously been investigated in some detail for hard X-ray photons [18]. Eq. (5) predicts a cross section of 4.4×10^{-51} cm^4 s at 284.18 eV. However, as we are on a resonance the equation is likely not applicable as it does not account for resonance effects and these could play an indeterminate role here. As the difference between the binding energy and the laser energy is small, minute laser energy fluctuations will have large impacts on the cross section and may have an unknown effect on the absolute value of this cross section. As such the absolute measured value should be viewed with some caution. Here the observed

laser energy fluctuations are estimated at 0.03 eV, and the spectral width can be large as 0.5% of the central energy. These fluctuations are enough to result in a certain fraction of the photons to be above resonance, likely lowering the two-photon absorption cross section reported here significantly [27]. The two-photon absorption cross section at 260.49 eV and 307.86 eV cannot be determined from these measurements due to low signal to noise ratios, but it is at least three orders of magnitude lower than what is observed at 284.18 eV.

In monitoring transmission, these measurements are inherently sensitive to a variety of nonlinear processes and can be used above the absorption edge. At energies well above the edge, X-ray induced transparency is another possible phenomenon [33]. This would manifest as an increase in transmission at high intensity in Fig. 2C, but was not observed for the intensity range investigated here.

4. Conclusions

Transmission measurements of soft X-ray free electron laser pulses through graphite were made near the carbon K-edge. At energies 25 eV above or below the K-edge absorption onset, the FEL behaves primarily as a linear absorption probe. Near the edge, significant two-photon absorption is observed, and is several orders of magnitude larger than would be predicted if not at resonance. This result has significant implications for future time-resolved XAS studies utilizing FEL probes, as such measurements will need to account for the effects of TPA if conducted in a transmission geometry. The observed two-photon cross section ($\sim 6 \times 10^{-48}\,\mathrm{cm}^4\,\mathrm{s}$) is similar to trends from previous measurements.

Acknowledgments

TPA measurements were conducted at the EIS-TIMEX beamline at FERMI. R.K.L., A.M.R, J.W.S., and R.J.S were supported by the Office of Science, Office of Basic Energy Sciences, Division of Chemical Sciences, Geosciences, and Biosciences of the US Department of Energy at the Lawrence Berkeley National Laboratory (LBNL) under Contract No. DE-AC02-05CH11231. C.J.H. and S.L.R. were supported by the U. S. Army Research Laboratory (ARL) and the U. S. Army Research Office (ARO) under contract/grant number W911NF-13-1-0483 and W911NF-17-1-0163. S.L.R. received a National Science Foundation Graduate Research Fellowship under Grant No. DGE 1106400. Any opinions, findings, and conclusions or recommendations expressed in this material are those of the author(s) and do not necessarily reflect the views of the National Science Foundation. N.F., P.M., M.C., and L.P. were supported by the project "Single-shot X-ray emission-spectroscopy experiments," funded by the Italian Ministry for Education and Research as In-Kind Project for the EuroFEL consortium. W.S.D. was supported by the Joint Center for Artificial Photosynthesis, a DOE Energy Innovation Hub, supported through the Office of Science of the U.S. Department of Energy under Award Number DE-SC0004993. S.T.C. was supported by U.S. Department of Energy under Contract No. DE-AC36-08-GO28308 with the National Renewable Energy Laboratory. D.S., T-C.W., D.N., S.T.C. and C.P.S. were in part supported by U.S. Department of Energy, Office of Energy Efficiency & Renewable Energy, Solar Energy Technology Office BRIDGE program. D.S., T-C.W., D. N., and C.P.S. were also supported by the SLAC National Accelerator Laboratory, which is supported by the US Department of Energy, Office of Science, Office of Basic Energy Sciences under contract No. DE-AC02-76S00515. This work was supported by a user project at The Molecular Foundry (TMF), LBNL, which supported T.A.P. and D.P. TMF is supported by the Office of Science, Office of Basic Energy Sciences under the LBNL contract above. C.D.P. was supported by the of the U.S. Department of Energy, Office of Basic Energy Sciences, Division of Materials Sciences and Engineering, under Contract No. DE-AC02-76SF00515 through TIMES at SLAC. Material support was provided by the Office of Science, Office of Basic Energy Sciences, Division of Chemical Sciences, Geosciences, and Biosciences of the US Department of Energy under the LBNL contract above. Travel support was provided under the ARL and ARO contracts above.

References

[1] Y.R. Shen, The Principles of Nonlinear Optics, Wiley, New York, 1984.
[2] P.A. Franken, A.E. Hill, C.W. Peters, G. Weinreich, Generation of optical harmonics, Phys. Rev. Lett. 7 (1961) 118–119, https://doi.org/10.1103/PhysRevLett.7.118.
[3] J. Stöhr, NEXAFS Spectroscopy, Springer, Berlin, Heidelberg, 1992. https://doi.org/10.1007/978-3-662-02853-7.
[4] S. Mukamel, Principles of Nonlinear Optical Spectroscopy, Oxford University Press, New York, 1995.
[5] J. Als-Nielsen, D. McMorrow, Elements of Modern X-ray Physics, John Wiley & Sons Inc, Hoboken, NJ, USA, 2011. https://doi.org/10.1002/97811199983c65.
[6] C. Bostedt, S. Boutet, D.M. Fritz, Z. Huang, H.J. Lee, H.T. Lemke, A. Robert, W.F. Schlotter, J.J. Turner, G.J. Williams, Linac coherent light source: the first five years, Rev. Mod. Phys. 88 (2016) 15007, https://doi.org/10.1103/RevModPhys.88.015007.
[7] N. Rohringer, D. Ryan, R.A. London, M. Purvis, F. Albert, J. Dunn, J.D. Bozek, C. Bostedt, A. Graf, R. Hill, S.P. Hau-Riege, J.J. Rocca, Atomic inner-shell X-ray laser at 1.46 nanometres pumped by an X-ray free-electron laser, Nature 481 (2012) 488–491, https://doi.org/10.1038/nature10721.
[8] F. Bencivenga, R. Cucini, F. Capotondi, A. Battistoni, R. Mincigrucci, E. Giangrisostomi, A. Gessini, M. Manfredda, I.P. Nikolov, E. Pedersoli, E. Principi, C. Svetina, P. Parisse, F. Casolari, M.B. Danailov, M. Kiskinova, C. Masciovecchio, Four-wave mixing experiments with extreme ultraviolet transient gratings, Nature 520 (2015) 205–208, https://doi.org/10.1038/nature14341.
[9] S. Shwartz, M. Fuchs, J.B. Hastings, Y. Inubushi, T. Ishikawa, T. Katayama, D.A. Reis, T. Sato, K. Tono, M. Yabashi, S. Yudovich, S.E. Harris, X-ray second harmonic generation, Phys. Rev. Lett. 112 (2014) 163901, https://doi.org/10.1103/PhysRevLett.112.163901.
[10] R.K. Lam, S.L. Raj, T.A. Pascal, C.D. Pemmaraju, L. Foglia, A. Simoncig, N. Fabris, P. Miotti, C.J. Hull, A.M. Rizzuto, J.W. Smith, R. Mincigrucci, C. Masciovecchio, A. Gessini, E. Allaria, G. De Ninno, B. Diviacco, E. Roussel, S. Spampinati, G. Penco, S. Di Mitri, M. Trovò, M. Danailov, S.T. Christensen, D. Sokaras, T.-C. Weng, M. Coreno, L. Poletto, W.S. Drisdell, D. Prendergast, L. Giannessi, E. Principi, D. Nordlund, R.J. Saykally, C.P. Schwartz, Soft X-ray second harmonic generation as an interfacial probe, Phys. Rev. Lett. 120 (2018) 23901, https://doi.org/10.1103/PhysRevLett.120.023901.
[11] T.E. Glover, D.M. Fritz, M. Cammarata, T.K. Allison, S. Coh, J.M. Feldkamp, H. Lemke, D. Zhu, Y. Feng, R.N. Coffee, M. Fuchs, S. Ghimire, J. Chen, S. Shwartz, D. A. Reis, S.E. Harris, J.B. Hastings, X-ray and optical wave mixing, Nature 488 (2012) 603–608, https://doi.org/10.1038/nature11340.
[12] N.V. Tkachenko, Optical Spectroscopy: Methods and Instrumentations, Elsevier, 2006.
[13] W. Kaiser, C.G.B. Garrett, Two-photon excitation in CaF_2:Eu^{2+}, Phys. Rev. Lett. 7 (1961) 229–231, https://doi.org/10.1103/PhysRevLett.7.229.
[14] B.H. Cumpston, S.P. Ananthavel, S. Barlow, D.L. Dyer, J.E. Ehrlich, L.L. Erskine, A. A. Heikal, S.M. Kuebler, I.-Y.S. Lee, D. McCord-Maughon, J. Qin, H. Röckel, M. Rumi, X.-L. Wu, S.R. Marder, J.W. Perry, Two-photon polymerization initiators for three-dimensional optical data storage and microfabrication, Nature 398 (1999) 51, https://doi.org/10.1038/17989.
[15] F. Helmchen, W. Denk, Deep tissue two-photon microscopy, Nat. Methods 2 (2005) 932, https://doi.org/10.1038/nmeth818.
[16] S. Ghimire, M. Fuchs, J. Hastings, S.C. Herrmann, Y. Inubushi, J. Pines, S. Shwartz, M. Yabashi, D.A. Reis, Nonsequential two-photon absorption from the *K* shell in solid zirconium, Phys. Rev. A 94 (2016) 43418, https://doi.org/10.1103/PhysRevA.94.043418.
[17] K. Tamasaku, E. Shigemasa, Y. Inubushi, T. Katayama, K. Sawada, H. Yumoto, H. Ohashi, H. Mimura, M. Yabashi, K. Yamauchi, T. Ishikawa, X-ray two-photon absorption competing against single and sequential multiphoton processes, Nat. Photonics 8 (2014) 313–316, https://doi.org/10.1038/nphoton.2014.10.
[18] J. Szlachetko, J. Hoszowska, J.-C. Dousse, M. Nachtegaal, W. Błachucki, Y. Kayser, J. Sà, M. Messerschmidt, S. Boutet, G.J. Williams, C. David, G. Smolentsev, J.A. van Bokhoven, B.D. Patterson, T.J. Penfold, G. Knopp, M. Pajek, R. Abela, C.J. Milne, Establishing nonlinearity thresholds with ultraintense X-ray pulses, Sci. Rep. 6 (2016) 33292, https://doi.org/10.1038/srep33292.
[19] G. Doumy, C. Roedig, S.-K. Son, C.I. Blaga, A.D. DiChiara, R. Santra, N. Berrah, C. Bostedt, J.D. Bozek, P.H. Bucksbaum, J.P. Cryan, L. Fang, S. Ghimire, J.M. Glownia, M. Hoener, E.P. Kanter, B. Krässig, M. Kuebel, M. Messerschmidt, G.G. Paulus, D.A. Reis, N. Rohringer, L. Young, P. Agostini, L.F. DiMauro, Nonlinear atomic response to intense ultrashort x rays, Phys. Rev. Lett. 106 (2011) 83002, https://doi.org/10.1103/PhysRevLett.106.083002.

[20] H. Hasegawa, E.J. Takahashi, Y. Nabekawa, K.L. Ishikawa, K. Midorikawa, Multiphoton ionization of He by using intense high-order harmonics in the soft-x-ray region, Phys. Rev. A 71 (2005) 23407, https://doi.org/10.1103/PhysRevA.71.023407.
[21] E. Karule, On the evaluation of transition matrix elements for multiphoton processes in atomic hydrogen, J. Phys. B At. Mol. Phys. 4 (1971) L67–L70, https://doi.org/10.1088/0022-3700/4/9/014.
[22] S. Klarsfeld, Two-photon ionization of atomic hydrogen in the ground state, Lett. Al Nuovo Cim. 3 (1970) 395–398, https://doi.org/10.1007/BF02819081.
[23] W. Zernik, Two-photon ionization of atomic hydrogen, Phys. Rev. 135 (1964) A51–A57, https://doi.org/10.1103/PhysRev.135.A51.
[24] A. Simoncig, R. Mincigrucci, E. Principi, F. Bencivenga, A. Calvi, L. Foglia, G. Kurdi, L. Raimondi, M. Manfredda, N. Mahne, R. Gobessi, S. Gerusina, C. Fava, M. Zangrando, A. Matruglio, S. Dal Zilio, V. Masciotti, C. Masciovecchio, The EIS beamline at the seeded free-electron laser FERMI, in: A. Klisnick, C.S. Menoni (Eds.), Proc. SPIE, 2017, pp. 102430L. doi:10.1117/12.2268152.
[25] C. Masciovecchio, A. Battistoni, E. Giangrisostomi, F. Bencivenga, E. Principi, R. Mincigrucci, R. Cucini, A. Gessini, F. D'Amico, R. Borghes, M. Prica, V. Chenda, M. Scarcia, G. Gaio, G. Kurdi, A. Demidovich, M.B. Danailov, A. Di Cicco, A. Filipponi, R. Gunnella, K. Hatada, N. Mahne, L. Raimondi, C. Svetina, R. Godnig, A. Abrami, M. Zangrando, EIS: the scattering beamline at FERMI, J. Synchrotron Radiat. 22 (2015) 553–564, https://doi.org/10.1107/S1600577515003380.
[26] E. Allaria, R. Appio, L. Badano, W.A. Barletta, S. Bassanese, S.G. Biedron, A. Borga, E. Busetto, D. Castronovo, P. Cinquegrana, S. Cleva, D. Cocco, M. Cornacchia, P. Craievich, I. Cudin, G. D'Auria, M. Dal Forno, M.B. Danailov, R. De Monte, G. De Ninno, P. Delgiusto, A. Demidovich, S. Di Mitri, B. Diviacco, A. Fabris, R. Fabris, W. Fawley, M. Ferianis, E. Ferrari, S. Ferry, L. Froehlich, P. Furlan, G. Gaio, F. Gelmetti, L. Giannessi, M. Giannini, R. Gobessi, R. Ivanov, E. Karantzoulis, M. Lonza, A. Lutman, B. Mahieu, M. Milloch, S.V. Milton, M. Musardo, I. Nikolov, S. Noe, F. Parmigiani, G. Penco, M. Petronio, L. Pivetta, M. Predonzani, F. Rossi, L. Rumiz, A. Salom, C. Scafuri, C. Serpico, P. Sigalotti, S. Spampinati, C. Spezzani, M. Svandrlik, C. Svetina, S. Tazzari, M. Trovo, R. Umer, A. Vascotto, M. Veronese, R. Visintini, M. Zaccaria, D. Zangrando, M. Zangrando, Highly coherent and stable pulses from the FERMI seeded free-electron laser in the extreme ultraviolet, Nat. Photonics 6 (2012) 699–704, https://doi.org/10.1038/nphoton.2012.233.
[27] E. Allaria, D. Castronovo, P. Cinquegrana, P. Craievich, M. Dal Forno, M.B. Danailov, G. D'Auria, A. Demidovich, G. De Ninno, S. Di Mitri, B. Diviacco, W.M. Fawley, M. Ferianis, E. Ferrari, L. Froehlich, G. Gaio, D. Gauthier, L. Giannessi, R. Ivanov, B. Mahieu, N. Mahne, I. Nikolov, F. Parmigiani, G. Penco, L. Raimondi, C. Scafuri, C. Serpico, P. Sigalotti, S. Spampinati, C. Spezzani, M. Svandrlik, C. Svetina, M. Trovo, M. Veronese, D. Zangrando, M. Zangrando, Two-stage seeded soft-X-ray free-electron laser, Nat. Photonics 7 (2013) 913–918, https://doi.org/10.1038/nphoton.2013.277.
[28] M. Zangrando, D. Cocco, C. Fava, S. Gerusina, R. Gobessi, N. Mahne, E. Mazzucco, L. Raimondi, L. Rumiz, C. Svetina, Recent results of PADReS, the Photon Analysis Delivery and REduction System, from the FERMI FEL commissioning and user operations, J. Synchrotron Radiat. 22 (2015) 565–570, https://doi.org/10.1107/S1600577515004580.
[29] P. Finetti, H. Höppner, E. Allaria, C. Callegari, F. Capotondi, P. Cinquegrana, M. Coreno, R. Cucini, M.B. Danailov, A. Demidovich, G. De Ninno, M. Di Fraia, R. Feifel, E. Ferrari, L. Fröhlich, D. Gauthier, T. Golz, C. Grazioli, Y. Kai, G. Kurdi, N. Mahne, M. Manfredda, N. Medvedev, I.P. Nikolov, E. Pedersoli, G. Penco, O. Plekan, M.J. Prandolini, K.C. Prince, L. Raimondi, P. Rebernik, R. Riedel, E. Roussel, P. Sigalotti, R. Squibb, N. Stojanovic, S. Stranges, C. Svetina, T. Tanikawa, U. Teubner, V. Tkachenko, S. Toleikis, M. Zangrando, B. Ziaja, F. Tavella, L. Giannessi, Pulse duration of seeded free-electron lasers, Phys. Rev. X 7 (2017) 21043, https://doi.org/10.1103/PhysRevX.7.021043.
[30] L. Poletto, F. Frassetto, P. Miotti, A. Di Cicco, P. Finetti, C. Grazioli, F. Iesari, A. Kivimäki, S. Stagira, M. Coreno, Spectrometer for X-ray emission experiments at FERMI free-electron-laser, Rev. Sci. Instrum. 85 (2014) 103112, https://doi.org/10.1063/1.4898315.
[31] S. Schreck, M. Beye, J.A. Sellberg, T. McQueen, H. Laksmono, B. Kennedy, S. Eckert, D. Schlesinger, D. Nordlund, H. Ogasawara, R.G. Sierra, V.H. Segtnan, K. Kubicek, W.F. Schlotter, G.L. Dakovski, S.P. Moeller, U. Bergmann, S. Techert, L. G.M. Pettersson, P. Wernet, M.J. Bogan, Y. Harada, A. Nilsson, A. Föhlisch, Reabsorption of soft X-ray emission at high X-ray free-electron laser fluences, Phys. Rev. Lett. 113 (2014) 153002, https://doi.org/10.1103/PhysRevLett.113.153002.
[32] B.L. Henke, E.M. Gullikson, J.C. Davis, X-Ray interactions: photoabsorption, scattering, transmission, and reflection at E = 50–30,000 eV, Z = 1–92, At. Data Nucl. Data Tables 54 (1993) 181–342, https://doi.org/10.1006/adnd.1993.1013.
[33] B. Nagler, U. Zastrau, R.R. Fäustlin, S.M. Vinko, T. Whitcher, A.J. Nelson, R. Sobierajski, J. Krzywinski, J. Chalupsky, E. Abreu, S. Bajt, T. Bornath, T. Burian, H. Chapman, J. Cihelka, T. Döppner, S. Düsterer, T. Dzelzainis, M. Fajardo, E. Förster, C. Fortmann, E. Galtier, S.H. Glenzer, S. Göde, G. Gregori, V. Hajkova, P. Heimann, L. Juha, M. Jurek, F.Y. Khattak, A.R. Khorsand, D. Klinger, M. Kozlova, T. Laarmann, H.J. Lee, R.W. Lee, K.-H. Meiwes-Broer, P. Mercere, W.J. Murphy, A. Przystawik, R. Redmer, H. Reinholz, D. Riley, G. Röpke, F. Rosmej, K. Saksl, R. Schott, R. Thiele, J. Tiggesbäumker, S. Toleikis, T. Tschentscher, I. Uschmann, H. J. Vollmer, J.S. Wark, Turning solid aluminium transparent by intense soft X-ray photoionization, Nat. Phys. 5 (2009) 693–696, https://doi.org/10.1038/nphys1341.